



Laser-Based Ignition for a Gunfire Simulator (GUFS): Thermal Transport Properties for Candidate Igniter Materials

by M. J. McQuaid, A. E. Kinkennon,
R. A. Pesce-Rodriguez, and R. A. Beyer

ARL-TR-2033

August 1999

Approved for public release; distribution is unlimited.

The findings in this report are not to be construed as an official Department of the Army position unless so designated by other authorized documents.

Citation of manufacturer's or trade names does not constitute an official endorsement or approval of the use thereof.

Destroy this report when it is no longer needed. Do not return it to the originator.

Army Research Laboratory

Aberdeen Proving Ground, MD 21005-5066

ARL-TR-2033

August 1999

Laser-Based Ignition for a Gunfire Simulator (GUFS): Thermal Transport Properties for Candidate Igniter Materials

M. J. McQuaid, A. E. Kinkennon, R. A. Pesce-Rodriguez, and
R. A. Beyer

Weapons and Materials Research Directorate, ARL

Abstract

This report presents the results of a study undertaken to help build a database and modeling capability that will support the design of a laser-based ignition system for a gun-fire simulation (GUFS) platform. In this study, the thermal transport properties of pressed pellets of candidate igniter materials were experimentally investigated in the range 20–100° C via (1) the technique developed by Miller and Kotlar ("Technique for Measuring Thermal Diffusivity/Conductivity of Small Thermal Insulator Specimens," *Review of Scientific Instruments*, vol. 64, p. 2954, 1993) and (2) a small modification to their technique that allows it to be used for (slightly) electrically conductive materials. The compounds investigated in this manner include black powder, red powder (with and without 0.5-weight-percent carbon black), B/KNO₃, A1A, Zr/KClO₄, Ti/KClO₄, an ARCO formulation (with 0.5-weight-percent carbon black), and an FeO/Ti/Zr/NC mixture. In addition, the heat capacities of these compounds were determined over the range 20–100° C via differential scanning calorimetry. The experimentally derived parameters are employed as input to a simplified model of the heat-transfer process attending the irradiation of a candidate with a relatively low-fluence laser beam. The results indicate that the differences in the thermal transport properties of the materials studied will not lead to significant differences in the irradiance required to ignite them.

Acknowledgments

The authors are indebted to Dr. Martin Miller for the use of his experimental apparatus, his advice regarding its operation, and his help in interpreting the experimental results. The authors are also grateful for the help of Dr. Anthony Kotlar, who explained the interdependence of parameters in the model employed to fit the experimental data and who reviewed this report. Dr. Stephen Howard also reviewed this report and provided helpful comments. Gary Chen (U.S. Army Armament Research, Development, and Engineering Center [ARDEC]) provided the pyrotechnic pellets employed as samples in the study.

INTENTIONALLY LEFT BLANK.

Table of Contents

| | <u>Page</u> |
|------------------------------------------------------------------------------|-------------|
| Acknowledgments..... | iii |
| List of Figures | vii |
| List of Tables | ix |
| 1. Introduction | 1 |
| 2. Description of Igniter Materials..... | 3 |
| 3. Experimental Considerations..... | 4 |
| 4. Experimental Results | 12 |
| 5. Influence of Thermal Transport Properties on Irradiance Requirements..... | 15 |
| 6. Summary | 19 |
| 7. References | 21 |
| List of Symbols | 23 |
| Distribution List | 25 |
| Report Documentation Page | 27 |

INTENTIONALLY LEFT BLANK.

List of Figures

| <u>Figure</u> | <u>Page</u> |
|--------------------------------------------------------------------------------------------------------------------------------------------------------------------------------------------------------------------------------|-------------|
| 1. Schematic Diagram of Experimental Configuration Developed by MK [2] | 5 |
| 2. Schematic Diagram of Experimental Setup Employed for This Study..... | 8 |
| 3. Comparison of Experimentally Measured Values of the Heat Capacity of Fused Silica and the Recommendation of Reference [7]..... | 11 |
| 4. DSC Measurements of the Heat Capacity of Black Powder for Temperatures From 20 to 100° C | 12 |
| 5. DSC Measurements of the Heat Capacity of B/KNO ₃ for Temperatures From 20 to 100° C and an Estimate Based on Literature Values for the Constituents..... | 12 |
| 6. DSC Measurements of the Heat Capacity of Red Powder for Temperatures From 20 to 100° C | 13 |
| 7. DSC Measurements of the Heat Capacity of Red Powder With 0.5 Weight-Percent Added Carbon Black for Temperatures From 20 to 100° C | 13 |
| 8. DSC Measurements of the Heat Capacity of Zr/KClO ₄ for Temperatures From 20 to 100° C and an Estimate Based on Literature Values for the Constituents..... | 13 |
| 9. DSC Measurements of the Heat Capacity of Ti/KClO ₄ for Temperatures From 20 to 100° C and an Estimate Based on Literature Values for the Constituents..... | 13 |
| 10. DSC Measurements of the Heat Capacity of FeO/Ti/Zr/NC for Temperatures From 20 to 100° C and an Estimate Based on Literature Values for the Constituents..... | 14 |
| 11. DSC Measurements of the Heat Capacity of A1A for Temperatures From 20 to 100° C | 14 |
| 12. DSC Measurements of the Heat Capacity of an ARCO Formulation With 0.5-Weight-Percent Added Carbon Black for Temperatures From 20 to 100° C..... | 14 |
| 13. Comparison of $(\lambda_s \rho_s c_{ps})^{1/2}$ for Black Powder, B/KNO ₃ , Ti/KClO ₄ , Zr/KClO ₄ , FeO/Zr/Ti/NC, and an ARCO Formulation With 0.5-Weight-Percent Added Carbon Black..... | 16 |

| <u>Figure</u> | <u>Page</u> |
|----------------------------------------------------------------------------------------------------------------------------------------|-------------|
| 14. Thermal Diffusivity and Thermal Conductivity Measurements for Black Powder .. | 17 |
| 15. Thermal Diffusivity and Thermal Conductivity Measurements for B/KNO ₃ | 17 |
| 16. Thermal Diffusivity and Thermal Conductivity Measurements for Zr/KClO ₄ | 17 |
| 17. Thermal Diffusivity and Thermal Conductivity Measurements for Ti/KClO ₄ | 17 |
| 18. Thermal Diffusivity and Thermal Conductivity Measurements for an ARCO Formulation With 5-Weight-Percent Added Carbon Black..... | 18 |
| 19. Thermal Diffusivity and Thermal Conductivity Measurements for FeO/Ti/Zr/NC..... | 18 |

List of Tables

| <u>Table</u> | <u>Page</u> |
|----------------------------------------------------------------------------------|-------------|
| 1. Pyrotechnic Compositions and Some of Their Properties | 4 |
| 2. Comparison of Thermal Transport Property Measurements at 23.5° C..... | 18 |
| 3. Minimum Fluence Required to Reach Autoignition Temperature Within 0.5 s | 20 |

INTENTIONALLY LEFT BLANK.

1. Introduction

Laser-based ignition is being proposed as a means of improving the safety of rounds employed with a gun fire simulator (GUFS) system. The system platform carries 20 flash-and/or boom-producing rounds that produce threat cues and target “hit and kill” recognition during training exercises. The current rounds are initiated via electric matches, and, as with all such igniters, they are susceptible to inadvertent ignition by electrostatic discharge (ESD) and electromagnetic radiation (ER). A number of incidents involving GUFS platform rounds have been reported, and the risk that these munitions may inadvertently ignite will become increasingly acute as more and more ER-based sensors probe the modern battlefield and (by extension) training exercises. Laser-based ignition systems are immune to ER effects, and back-fitting the GUFS platform with such a system would reduce the safety hazard associated with the rounds. However, though there is little doubt that a workable laser-based ignition system could be built, the cost to do so is a concern. (Current guidance is, that to be tenable, the cost/round must be kept near current levels.) The work reported here represents part of an effort to develop a database and modeling capability that will facilitate the design of a cost-effective system.

Design options being considered for the GUFS application include (1) having a dedicated laser diode for each round on the platform (20 lasers total) or (2) having a single laser diode (or a solid-state laser) coupled to each round through an optical switch (one laser, one optical switch). Regardless of the approach chosen, the cost of the system will be driven by requirements for laser power, optical component quality, and mechanical tolerances—all of which depend on the minimum irradiance (intensity/spot size) necessary to properly function a round. The minimum irradiance, in turn, depends on the time available between the arrival of a trigger signal and the ignition event (i.e., ignition delay) and the mechanism(s) relevant to ignition on that time scale. In the case of GUFS platform rounds, ignition delays of up to 0.5 s are permissible. This time scale allows relatively low laser fluences to be employed, and the fluence will act simply as a heat (flux) source that raises the temperature of the igniter material until self-propagating chemical reactions ensue.

A simplified, one-dimensional (1-D) governing equation for the spatial (x) and temporal (t) dependence of the temperature, $T(x,t)$, in a material under such flux conditions is [1],

$$\frac{\partial T}{\partial t} = \alpha \frac{\partial^2 T}{\partial x^2} - \frac{1}{\rho c_p} \frac{\partial(f_o \exp(-nx))}{\partial x} + \frac{Qz}{c_p} \exp(-E/RT). \quad (1)$$

The first term on the right-hand side of this equation is associated with the diffusion of heat due to temperature gradients, the dynamics of which depend on the material's thermal diffusivity (α). (The thermal conductivity [λ] of a material is related to its thermal diffusivity per,

$$\alpha = \frac{\lambda}{\rho c_p}, \quad (2)$$

where ρ is the material's density and c_p is its heat capacity at constant pressure.) The second term on the right-hand side of equation (1) is associated with the absorption of radiant energy by the material, the dynamics of which depend on the incident flux (f_o) and the material's absorption coefficient (n). The last term is associated with chemical energy production, with the given function being the Arrhenius form of the heat release rate. The parameters of this function are the activation energy (E), a first-order pre-exponential factor (z), and the heat of reaction (Q). R is a constant.

Unfortunately, even this simplified model requires a plethora of parameters that are not generally available, making it difficult to identify systems with potentially low-fluence requirements. The work presented in this report is concerned with the thermal transport properties of various igniter materials and the influence thermal diffusion will have in determining the minimum fluence required to initiate these materials. Presented are the results of experiments conducted to establish the thermal transport properties of nine pyrotechnic compounds over the range 20–100° C. Most measurements were made with a slightly modified version of the experimental technique developed by Miller and Kotlar (MK) [2], the modified experiment yielding a measurement for the parameter $(\lambda_s \rho_s c_{ps})^{1/2}$. In the interest of establishing

λ and α from these measurements, heat capacities for all of the compounds were determined for the range 20–100° C via differential scanning calorimetry. To simulate the temperature response of the candidates to relatively low-level laser fluences, the experimental values were employed as parameters in a 1-D heat-transfer model that assumes $n = \infty$ and $Q = 0$, and the irradiance required to raise the compound's surface to its autoignition temperature within 0.5 s is calculated. The results indicate that the differences in the thermal transport properties of the candidate materials (alone) will not lead to significant differences in the irradiance required to ignite them.

2. Description of Igniter Materials

Table 1 shows the chemical compositions and some of the physical properties of the igniter materials identified by the U.S. Army Armament Research, Development, and Engineering Center (ARDEC) as candidates for the GUFS application. Except for red powder, all are "standard" pyrotechnics for which some degree of characterization exists in the open literature. Red powder is a patented ARDEC formulation that is being developed in conjunction with Thiokol. Lots M292 and M296 were doped with a small amount of carbon black. It is considered that such an additive may reduce the fluence required to ignite a material by increasing its optical density. However, it remains to be determined whether the dopant produces other effects, such as increasing the thermal conductivity, that negate this potential benefit.

All compounds employed in the experiments were prepared by ARDEC and provided to us as cylindrical pellets (0.65-cm diameter \times 0.65-cm length). The pellets were formed by pressing the mixtures to 152 MPa (22 kpsi). The pellets were friable, particularly those with high metal or metal oxide content, and care needed to be exercised in handling them. For most of the measurements reported here, the pellets were simply used as supplied. In cases where thinner specimens were employed (i.e., for the straight adaptation of the MK technique [2]), the pellets were wafered by inserting them into an acrylic tube and cutting the resulting assembly with a low-speed saw with a diamond-coated blade. In all of these cases, ethyl alcohol was employed

Table 1. Pyrotechnic Compositions and Some of Their Properties

| Lot No. ^a | Material ^b (weight-percent components) | Pellet Loading (MPa) | Density (g/cm ³) | Autoignition Temperature (°C) |
|----------------------|-------------------------------------------------------------------------|-------------------------|---------------------------------|--------------------------------------|
| M279 | Red Powder (PhPhK-15/KNO ₃ -75/S-10) | 152 | 1.86 | 450 |
| M291 | Zr/KClO ₄ /VAAR (Zr-50/KClO ₄ -50/VAAR-1) | 152 | 2.86 | 411 ^c |
| M292 | ARCO Powder w/ 0.5% Carbon Black | 152 | 1.74 | Unknown |
| M293 | Black Powder (C-15/KNO ₃ -75/S-10) | 152 | 1.74 | 464 ^d 200 ^d |
| M294 | B/KNO ₃ (B-25/KNO ₃ -75/VAAR-1) | 152 | 1.59 | 431 |
| M295 | Ti/KClO ₄ /VAAR (Ti-50/KClO ₄ -50/VAAR-1) | 152 | 2.34 | Unknown |
| M296 | Red Powder w/ 0.5% Carbon Black (PhPhK-15/KNO ₃ -75/S-10) | 152 | 1.85 | 450 |
| M297 | FeO/Ti/Zr/NC (FeO-50/Ti-32.5/Zr-17/NC-5) | 152 | 3.03 | 456 |
| SI163 | A1A (Zr-65/Fe ₂ O ₃ -25/DE-10/VAAR-1) | 152 | 3.18 | 427 |

^a ARDEC designation.

^b PhPhK = potassium salt of phenolphthalein, DE = diatomaceous earth, and VAAR = vinyl alcohol acetate resin.

^c Value is the material's explosive temperature, the autoignition temperature is unknown.

^d Two different autoignition values are reported for black powder.

as a cutting fluid. In some cases, the specimen's produced by wafering were sanded with 15- μ m grit paper to improve their surface planarity and finish. If wafered, the specimens were stored in an evacuated dessicator for at least 2 days prior to using them in an experiment.

3. Experimental Considerations

Except for minor variations, the experimental apparatus used in this study was the same as that developed and employed by MK [2]. MK have discussed the difficulty of measuring the thermal conductivity and thermal diffusivity of small solid samples, and their technique

addresses typical concerns such as the generation of a well-defined heat flux, the match between experimental and model boundary conditions, and instrumentation errors. A schematic diagram of their experiment is shown in Figure 1. The experiment involves resistively heating a 4.4-cm-long, 1.2-cm-wide, 0.0005-cm-thick Constantan foil (Hamilton Precision Metals) via a voltage-regulated power supply (Hewlett-Packard, Model 6024A), the circuit producing a step increase in current (and heat flux) when completed via a mercury-wetted relay. The heat flux sends thermal waves into the adjacent test sections, and the temperature response at a known distance from the foil is monitored with a bare Chromel/Alumel thermocouple (Omega, Style I or Style II). The output of the thermocouple is preamplified via a differential amplifier (Stanford Research Systems, Model SR560) and recorded by a digital oscilloscope (Nicolet, Model 4094/4570) over a 4- or 8-s period. One-tenth of the period is recorded prior to heat flux onset, providing an unbiased window on the test fixture temperature (T_0). A data point was acquired every 0.002 s for the 4-s duration experiments and every 0.004 s for the 8-s duration experiments. To determine the heat flux (f_0) generated by the foil, a nominal value for the current in the foil (I_0) was obtained from the readout of a multimeter (Fluke, Model 77) and the ($I^2 r_f$) heat generation was calculated using a previously measured value of the foil's resistance ($r_f = 0.34 \Omega$). The power supply was typically set to produce a current level in the range 1.5–2.5 A, with the resultant heat flux being in the range 0.14–0.40 W/cm². The temperature of the test fixture is controlled by circulating a 50/50 ethylene glycol-water mixture from a temperature-controlled bath (Neslab, Model ULT-80DD) through copper tubing soldered to the copper block housing the test fixture.

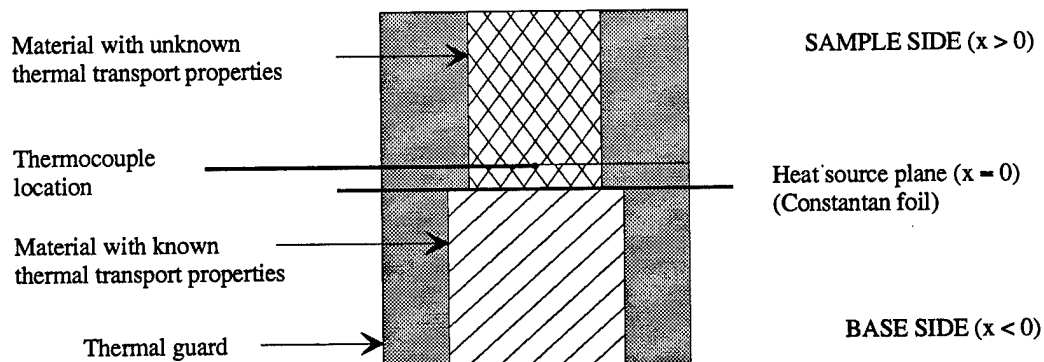


Figure 1. Schematic Diagram of Experimental Configuration Developed by MK [2].

MK have shown that their experiment approaches a mathematically idealized system in which a step function heat flux emanates from a plane between two semi-infinite media. The governing equation for this idealization is

$$\frac{\partial T}{\partial t} = \alpha \frac{\partial^2 T}{\partial x^2}, \quad (3a)$$

with boundary conditions

$$T(x,0) = T_o; -\infty < x < +\infty, \quad (3b)$$

$$\lambda_b \frac{\partial T(0^-,t)}{\partial x} = f^-(0^-,t); x < 0, \quad (3c)$$

$$\lambda_s \frac{\partial T(0^+,t)}{\partial x} = f^+(0^+,t); x > 0, \text{ and} \quad (3d)$$

$$T(0^+,t) = T(0^-,t), \quad (3e)$$

where x is the distance from the source plane and the subscripts s and b identify properties belonging to the sample and base, respectively. Conservation of energy requires that the sum of the heat fluxes going into the sample, $f^+(0^+,t)$, and the base, $f^-(0^-,t)$, be equal to the total flux emanating from the source plane, f_o . The solution to this system of equations [i.e., the temperature response of a point in the sample ($x > 0$)] is given by [3]

$$T = T_o + \left(\frac{2f_o \sqrt{\alpha_s \alpha_b t}}{\lambda_s \sqrt{\alpha_b} + \lambda_b \sqrt{\alpha_s}} \right) ierfc \left(\frac{x}{2\sqrt{\alpha_s t}} \right). \quad (4)$$

The last term on the right-hand side of equation (4) is the complementary error function integral

$$\text{ierfc}(z) = \sqrt{\frac{1}{\pi}} e^{-z^2} - \frac{2z}{\sqrt{\pi}} \int_z^\infty e^{-\xi^2} d\xi. \quad (5)$$

To derive α_s and λ_s , equation (4) is fit to the experimentally measured temperature response via a nonlinear least-squares-fitting routine. (The computation of the complex error function integral was accomplished by calculating the complex error function for the argument via the rational approximation suggested by Hui et al. [4] and making an appropriate transformation.) In performing a fit, all model parameters except α_s , λ_s , and T_o are set to measured values and the fitting routine allowed to vary α_s , λ_s , and T_o to minimize the root mean square of the residual. Being mathematically independent parameters, both α_s and λ_s are determined directly from this experiment.

It was found, however, that the MK technique could not be used to characterize the thermal transport properties of the FeO/Ti/Zr/NC compound [5]. During experiments with this compound, the thermocouple reading dropped precipitously at the instant the electrical heating pulse started. This suggested that current was leaking to the thermocouple, compromising not only the thermocouple output, but our ability to characterize the heat flux. This observation prompted us to consider monitoring the temperature response in the base. (See Figure 2.) Not only does this configuration resolve the problem posed by (slightly) electrically conductive materials such as FeO/Zr/Ti/NC, it offers operational advantages. It precludes the need to prepare thin samples, and it facilitates the testing of a series of samples because, once in place, the fragile thermocouple does not have to be handled again.

However, the benefits accrued through this approach come with a significant price—namely, that the function describing the temperature response becomes

$$T(x,t) = T_o + \frac{2f_o\sqrt{t}}{\lambda_b/\sqrt{\alpha_b} + \lambda_s/\sqrt{\alpha_s}} \text{ierfc}\left(\frac{x}{2\sqrt{\alpha_b t}}\right) \quad (6a)$$

or

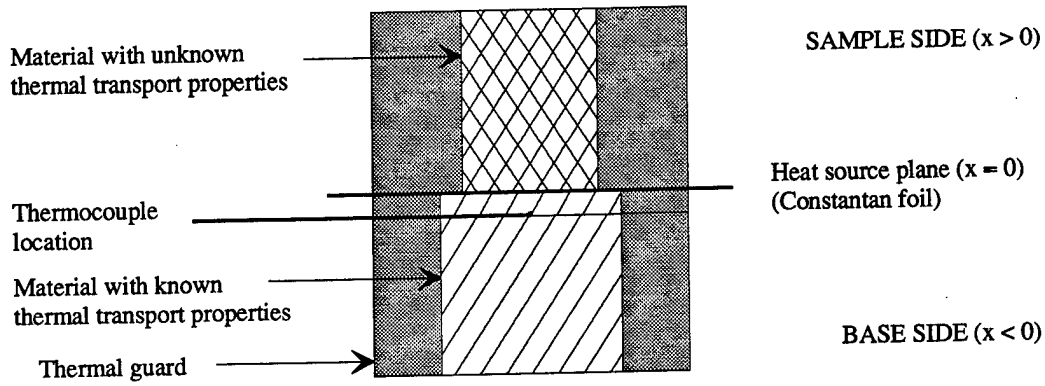


Figure 2. Schematic Diagram of Experimental Setup Employed for This Study.

$$T(x,t) = T_o + \frac{2f_o\sqrt{t}}{\sqrt{\lambda_b\rho_b c_{pb}} + \sqrt{\lambda_s\rho_s c_{ps}}} \text{ierfc}\left(\frac{x}{2\sqrt{\alpha_b t}}\right), \quad (6b)$$

and, in fitting this function to the experimental data, α_s and λ_s are no longer mathematically independent parameters. Instead, the parameter derivable from the experiment is $(\lambda_s\rho_s c_{ps})^{1/2}$. Thus a specimen's ρ and c_p must be known to get absolute values for λ_s and α_s . While the density is a relatively easy property to measure, heat-capacity measurements are a nontrivial extra step. Nevertheless, the Figure 2 configuration was used for most of the results reported here. To determine $(\lambda_s\rho_s c_{ps})^{1/2}$ from experiments with this configuration, nonlinear least-squares fits of equation (6b) to the experimental data were performed, all model parameters except $(\lambda_s\rho_s c_{ps})^{1/2}$ and T_o being set to measured values, and the program allowed to vary $(\lambda_s\rho_s c_{ps})^{1/2}$ and T_o to optimize the fit of the function to the data.

Another change we made to the basic technique developed by MK involved refining the temperature response model to account for the time constant of the thermocouple. This change was necessitated by the use of Style I thermocouples instead of Style II thermocouples to monitor the temperature at one juncture in this study. Though made from the same thickness of foil, Style I and Style II thermocouples have different geometries, and the time constant of Style I thermocouples ($t_c = 10 - 20$ ms) is longer than that of Style II thermocouples ($t_c = 2 - 5$ ms).

(The seller of the thermocouples defines the time constant simply as the time required for the thermocouple reading to transition 63.2% of an instantaneous temperature change.) The difference in time constants proved to be significant, with α and λ values derived from experiments with Style I and Style II thermocouples being different if the time constant was neglected. This is in contrast to the case examined by MK, who found that the results obtained using 5- and 12- μm -thick (Style II) thermocouples were the same and concluded that the time lag of the thermocouple response could be neglected. To incorporate the effect of the time constant into the data reduction model, it was assumed that the response of the thermocouple ($R(t)$) to a unit step increase in temperature was associated with the form

$$R(t) = 1 - \exp(-t/t_c) \quad (7)$$

and Duhamel's formula [6] was employed to express the response of the measurement system—the oscilloscope voltage reading, $u(t)$ —to the driving function $T(x,t)$ [i.e., equation (4) or (6b)]:

$$u(t) = \int_0^t R'(\tau)T(x,t-\tau)d\tau. \quad (8)$$

This equation was incorporated into the system model by calculating $R'(\tau)T(x,t-\tau)$ at 0.001-ms intervals for $0 < \tau < t$ and using Simpson's rule to evaluate the integral. Corrected in this manner, the results obtained with Style I and Style II thermocouples were brought into agreement.

It is also worth noting that fused silica was employed as the base material in most of the experiments. MK had employed acrylic as the base material, and the initial room-temperature results of this study were obtained with an acrylic base. However, acrylic's glass transition temperature is below 100° C, a value that we were interested in reaching. The decision to employ fused silica was based primarily on its availability and having had previous experience with it in this experiment. But, it is not an optimal choice. As noted by MK, the best measurements will be obtained when the thermal transport properties of the base and sample are

similar. [It is suggested that $(\lambda_s \rho_s c_{ps})^{1/2}$ be used in matching materials for this application.] The literature value of $(\lambda_s \rho_s c_{ps})^{1/2}$ for fused silica is about $0.14 \text{ J/cm}^2\text{-K-s}^{1/2}$, while, for the compounds studied here, this parameter was found to fall in the range $0.05\text{--}0.10 \text{ J/cm}^2\text{-K-s}^{1/2}$.

The values of α and λ for the base material, which are needed as input to the model of the heat-transfer process, were established experimentally by conducting tests in which the sample side was occupied by a specimen from the same lot as that used to construct the base. This configuration provides a direct, simultaneous measurement of α and λ without any *a priori* knowledge of these properties. Values for the fused silica base were obtained for the range $20\text{--}100^\circ \text{ C}$ and the linear least-squares fit of this data— $\lambda = 12.055 - 8.4 \times 10^{-5}T \text{ mW/cm-K}$, $\alpha = 7.6957 - 2.14 \times 10^{-2}T \text{ cm}^2/\text{s}$, where T is in degrees Celsius—was incorporated directly into the data-reduction model. These values are similar to those reported by MK [2].

Toward establishing α and λ for the pyrotechnic compounds from $(\lambda_s \rho_s c_{ps})^{1/2}$ values, heat-capacity measurements were made with a Mettler TA3000 differential scanning calorimeter (DSC). DSC measurements of heat capacity are based on comparing the electrical power needed to ramp (at a constant rate) the temperature of an empty (aluminum) pan and the same pan with a known mass of sample. For the results reported here, a sample of 10 to 15 mg was shaved from a pellet, introduced to the DSC, cooled to -30° C , then ramped at 10° C/min up to 110° C . After this measurement, the sample was “dried” by heating it at 100° C for approximately 1 hr with 5–10 ml/min of argon flowing through the chamber. The sample was then cooled back down, reweighed, and the measurement was repeated. Except where noted, the values reported in section 4 are derived from the second measurement on each sample. The values include a correction based on a temperature-dependent scaling factor derived from tests with sapphire specimens. (The scaling factor adjusts the DSC results for the sapphire specimens such that literature values are obtained.)

For the purpose of deriving λ and α from $(\lambda_s \rho_s c_{ps})^{1/2}$, the results for two different samples were averaged and a polynomial of the form

$$c_p(T) = a_0 + a_1T + a_2T^2 + a_3T^3 + \dots \quad (9)$$

fit to the average. The order of the polynomial employed to fit the data was based on our judgement as to a polynomial's ability to reproduce the data over the temperature range of interest and on using the lowest order polynomial possible.

It is also noted that the DSC measurements (should have) provided c_p values for the range -10 – 100°C . However, in all of the compounds studied, the measured c_p values dropped relatively rapidly with temperature for temperatures below 20°C . This trend was at odds with expectations for compounds whose c_p values could be estimated based on literature values for their constituents, prompting us to develop an independent experimental check of the DSC results. The check involved calculating c_p for the fused silica employed as the base in the test fixture from equation (2) using (1) values of α and λ found via the MK technique and (2) a separate measurement of density. As shown in Figure 3, the values derived from the two techniques are in good agreement for the range 20 – 100°C . They are, however, significantly below values recommended in the literature [7]. Thus, though we have some misgivings about the c_p results, the fused silica results and comparison with estimates for some of pyrotechnic compounds based on literature values for their constituents support their validity in the range 20 – 100°C . Also, since this range covers most of the thermal transport data collected, no effort was undertaken to reconcile the DSC c_p results and expectations for lower temperatures and the lower temperature results are not reported here.

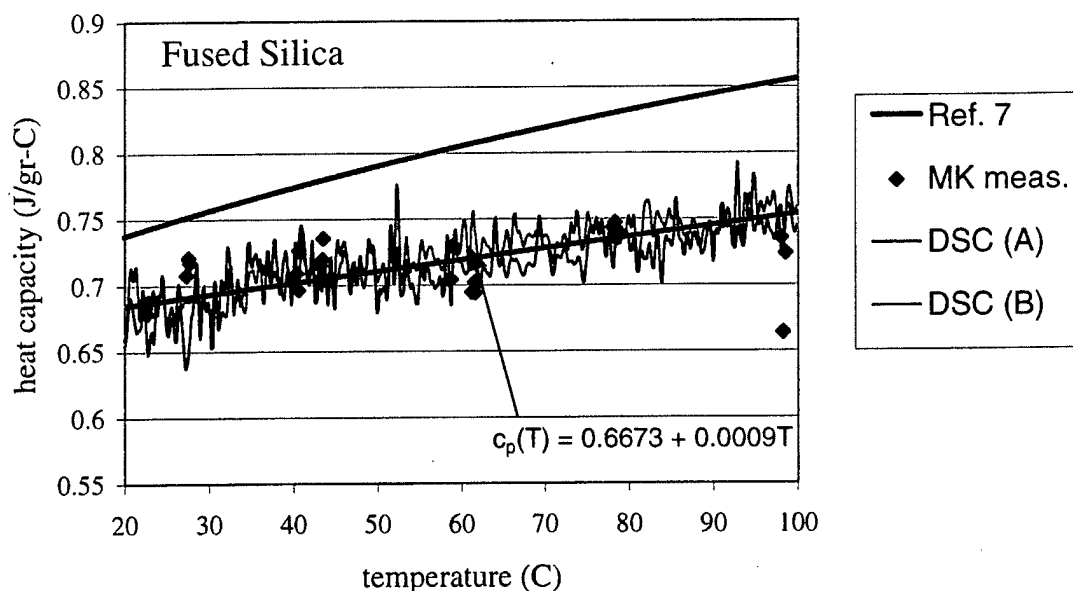


Figure 3. Comparison of Experimentally Measured Values of the Heat Capacity of Fused Silica and the Recommendation of Reference [7].

4. Experimental Results

Figures 4–12 show the experimentally determined heat capacities for the nine candidate compounds provided to us by ARDEC. In cases where the heat capacities of the constituents could be found in the literature [7], an estimate for the compound is provided for comparison. (The mass fractions of the constituents needed for these estimates are given in Table 1.) In the case of the compounds containing red powder (M279 and M296), the c_p values obtained from the first transient to 110° C are higher than those measured during the second transient. It was also found in these two cases that the mass of the sample was reduced on the order of 1% by the first measurement and drying period. (The mass loss produced by the second transient was negligible.) A comparison of the results (Figures 6 and 7) suggests that a gas-producing “reaction,” perhaps simply evaporation, onsets at about 50° C in these compounds.

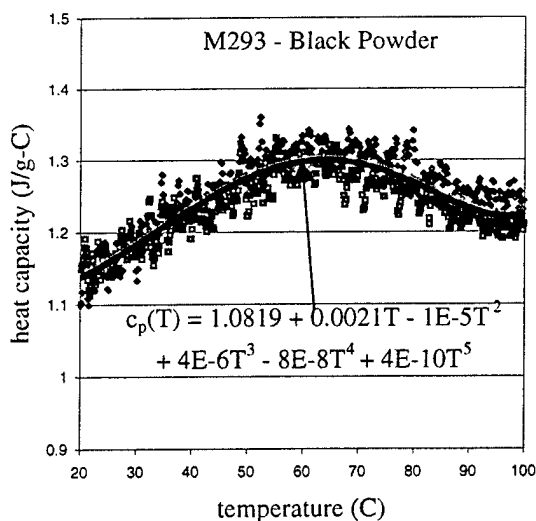


Figure 4. DSC Measurements of the Heat Capacity of Black Powder for Temperatures From 20 to 100° C.

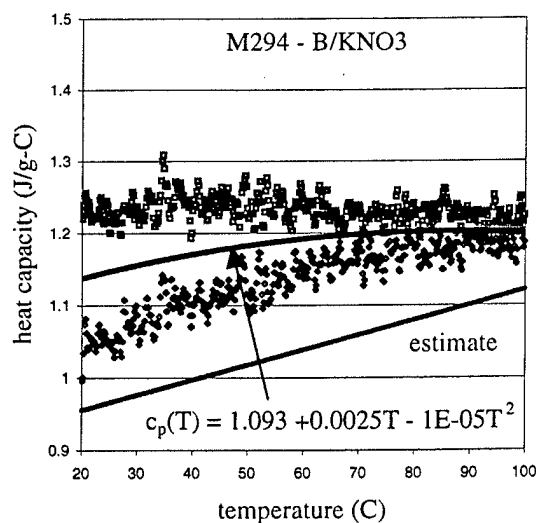


Figure 5. DSC Measurements of the Heat Capacity of B/KNO₃ for Temperatures From 20 to 100° C and an Estimate Based on Literature Values for the Constituents.

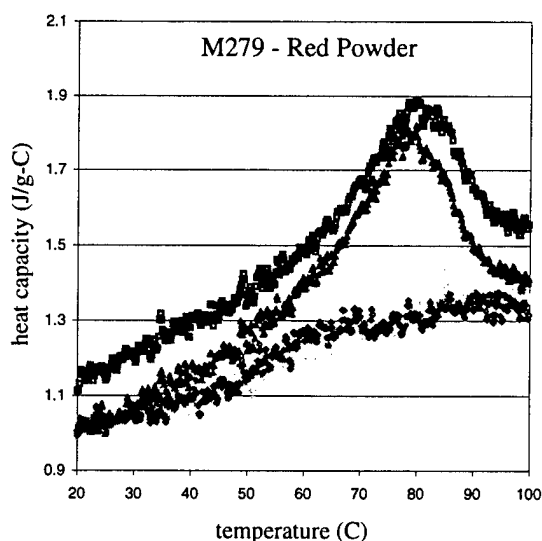


Figure 6. DSC Measurements of the Heat Capacity of Red Powder for Temperatures From 20 to 100° C. Comparison of Results Obtained Before and After Drying.

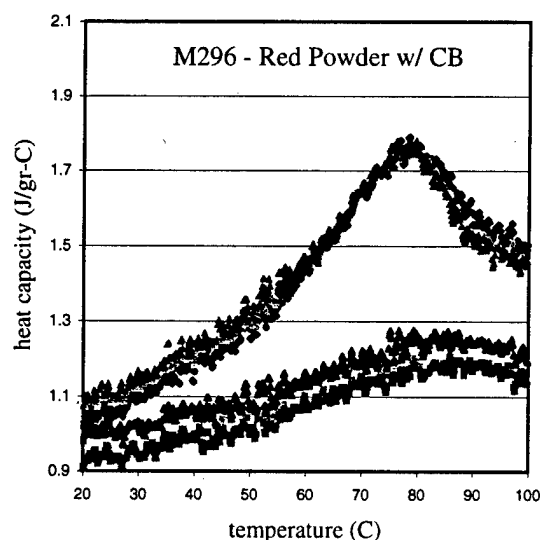


Figure 7. DSC Measurements of the Heat Capacity of Red Powder With 0.5-Weight-Percent Added Carbon Black for Temperatures From 20 to 100° C. Comparison of Results Obtained Before and After Drying.

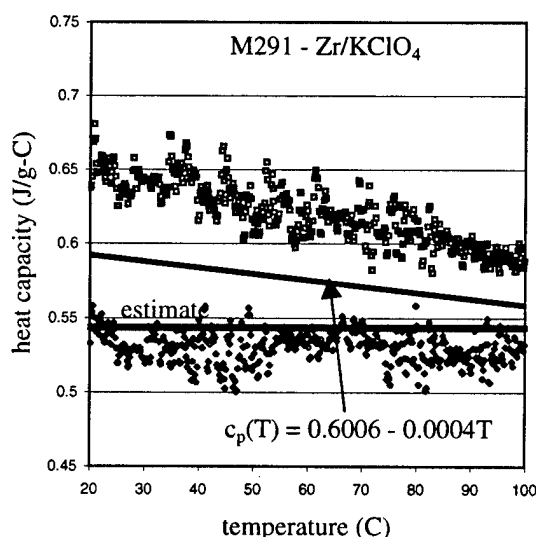


Figure 8. DSC Measurements of the Heat Capacity of Zr/KClO₄ for Temperatures From 20 to 100° C and an Estimate Based on Literature Values for the Constituents.

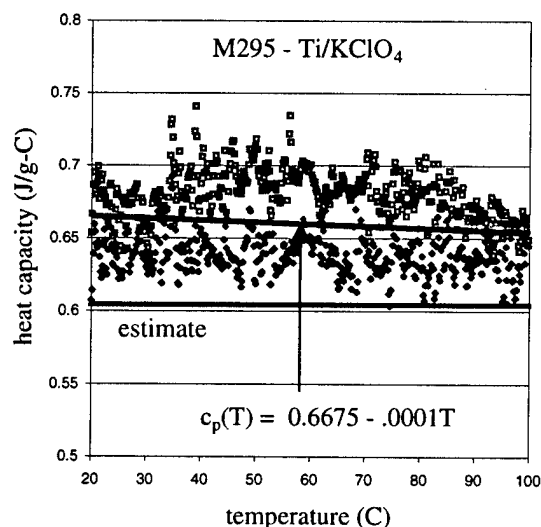


Figure 9. DSC Measurements of the Heat Capacity of Ti/KClO₄ for Temperatures From 20 to 100° C and an Estimate Based on Literature Values for the Constituents.

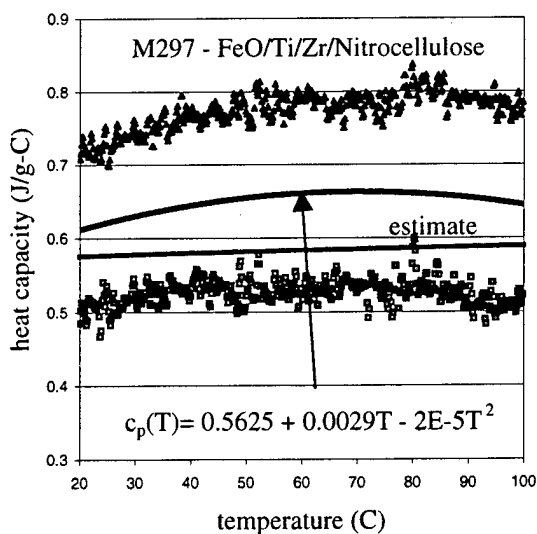


Figure 10. DSC Measurements of the Heat Capacity of FeO/Ti/Zr/NC for Temperatures From 20 to 100° C and an Estimate Based on Literature Values for the Constituents.

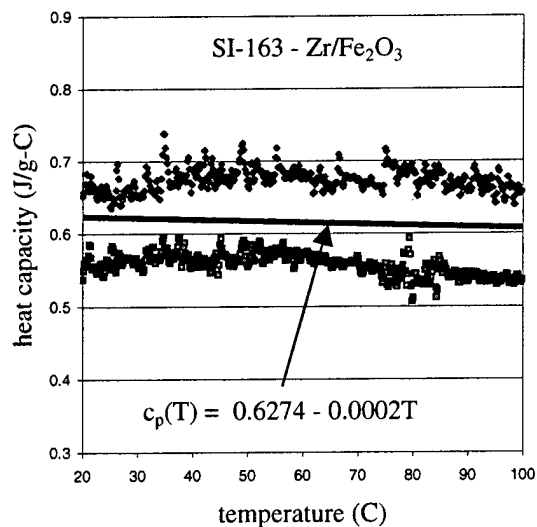


Figure 11. DSC Measurements of the Heat Capacity of A1A for Temperatures From 20 to 100° C.

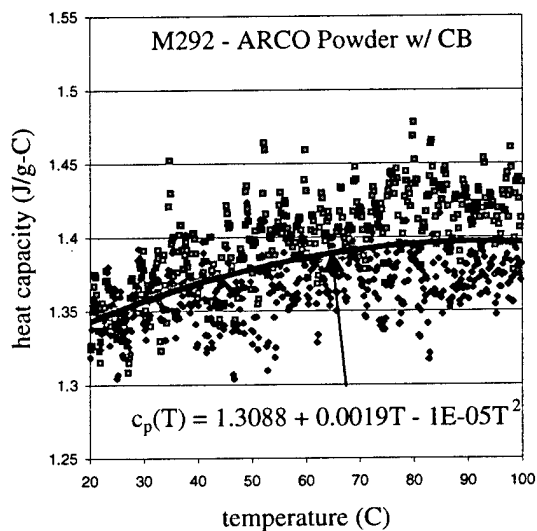


Figure 12. DSC Measurements of the Heat Capacity of an ARCO Formulation With 0.5-Weight-Percent Added Carbon Black for Temperatures From 20 to 100° C.

Figure 13 shows the values of $(\lambda_s \rho_s c_{ps})^{1/2}$ for six of the nine candidate compounds as determined from the modified version of the MK technique. Values are not provided for the two compounds with red powder (M279 and M296) or A1A (SI-163). Experiments were conducted with specimens containing red powder, but the results of the heat-capacity measurements, which show that their properties depend on their thermal history, argue against reducing the data and reporting the results. The A1A pellets proved to be very friable, and none of the specimens ended up being of sufficient quality to conduct the thermal transport property measurements. (The better pellets that we received were consumed in attempts to wafer them.) The reported values are observed to fall within a fairly narrow range that is bounded above by those for FeO/Ti/Zr/NC and below by those for Zr/KClO₄. The values are similar to that of acrylic (0.053 J/cm²-K-s^{1/2}) [2]. In all cases, $(\lambda_s \rho_s c_{ps})^{1/2}$ is observed to increase slightly with temperature over the range 20–100° C.

Figures 14–19 show the temperature-dependent values of α and λ for the six compounds as derived from the results with the modified (Figure 2) experimental configuration and the DSC heat-capacity measurements. A surprising result was the difference in property values obtained in this manner and values obtained earlier with the basic (Figure 1) configuration [5]. (See Table 2.) It is assumed that the discrepancies are associated with the fact that the compounds are slightly electrically conductive and that current leakage from the foil to the thermocouple impacts the temperature reading. Such an effect was obvious in the case of FeO/Ti/Zr/NC. It is presumed that the effect is just subtler for these other compounds.

5. Influence of Thermal Transport Properties on Irradiance Requirements

Equation (4) describes the temperature transient that occurs during low-fluence irradiation of a pyrotechnic pellet in contact with a flat, transparent window if (1) all of the incident radiation is absorbed at the surface of the pellet (i.e., $n = \infty$) and (2) energy production (or loss) due to chemical reactions or phase changes is negligible ($Q = 0$). Further noting that the complementary error function integral decreases as its argument increases, and thus that the

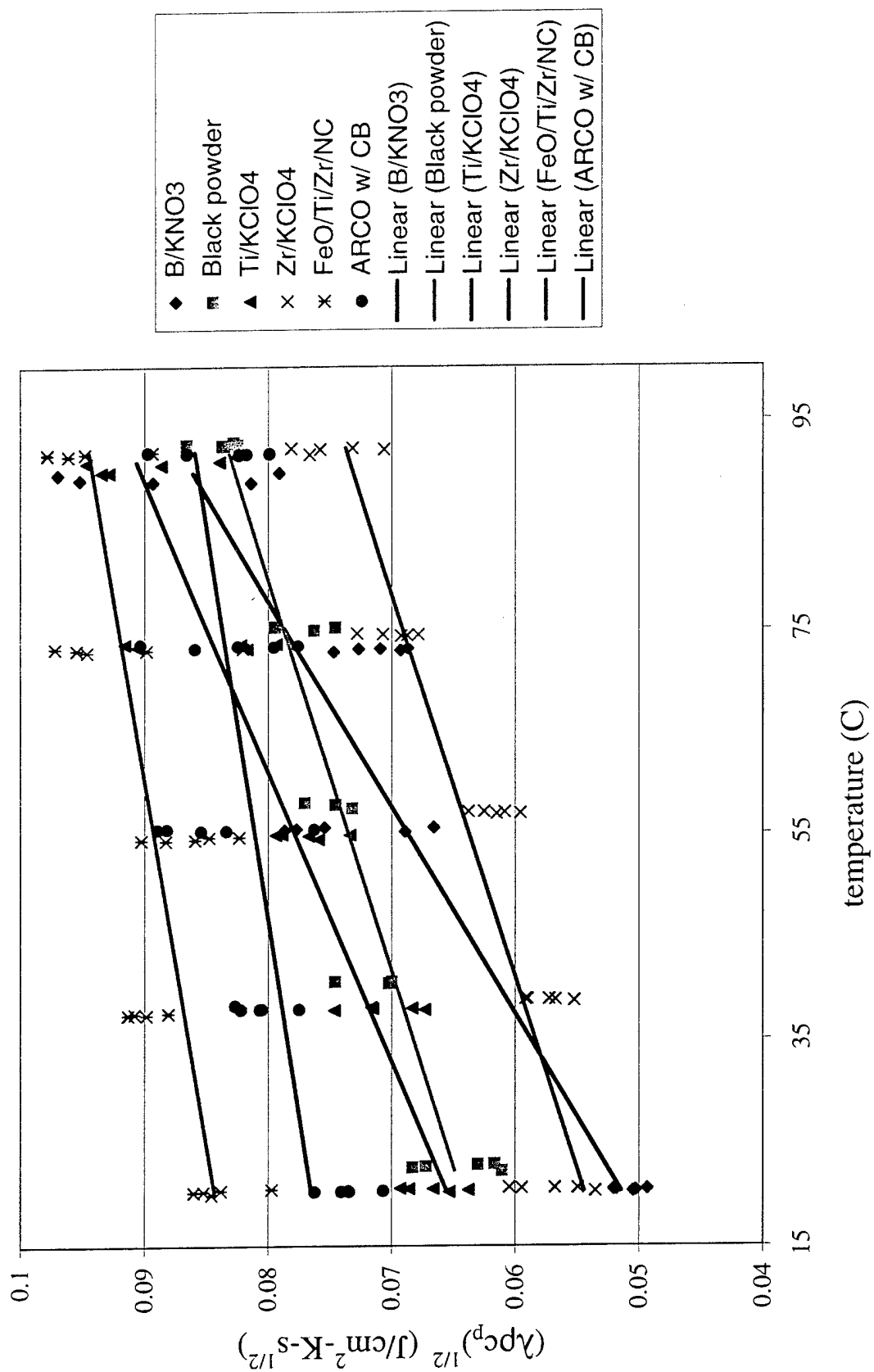


Figure 13. Comparison of $(\lambda \rho c_p)^{1/2}$ for Black Powder, B/KNO₃, Ti/KClO₄, Zr/KClO₄, FeO/Zr/Ti/NC, and an ARCO Formulation With 0.5-Weight-Percent Added Carbon Black.

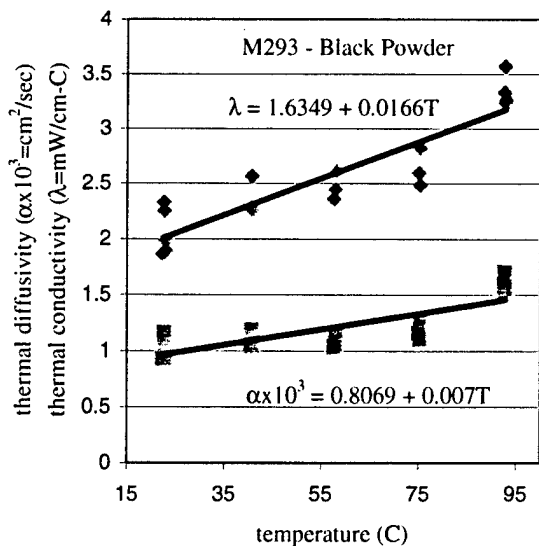


Figure 14. Thermal Diffusivity and Thermal Conductivity Measurements for Black Powder.

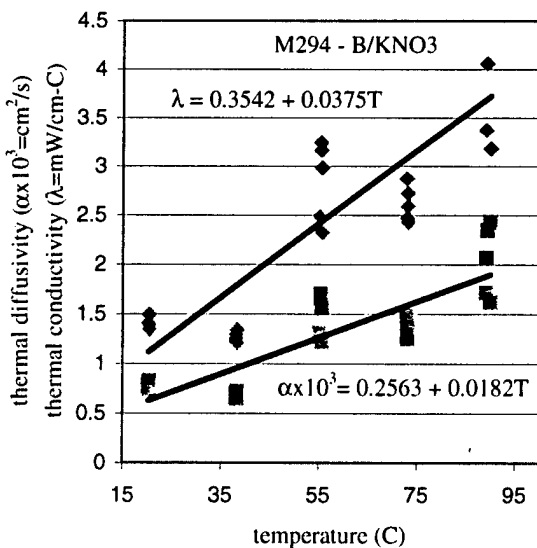


Figure 15. Thermal Diffusivity and Thermal Conductivity Measurements for B/ KNO_3 .

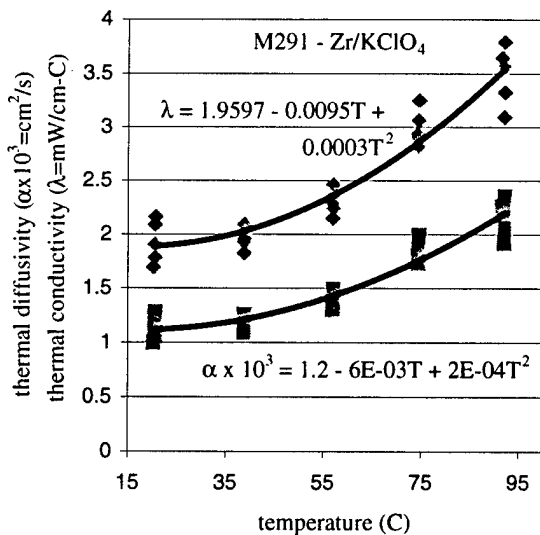


Figure 16. Thermal Diffusivity and Thermal Conductivity Measurements for Zr/ KClO_4 .

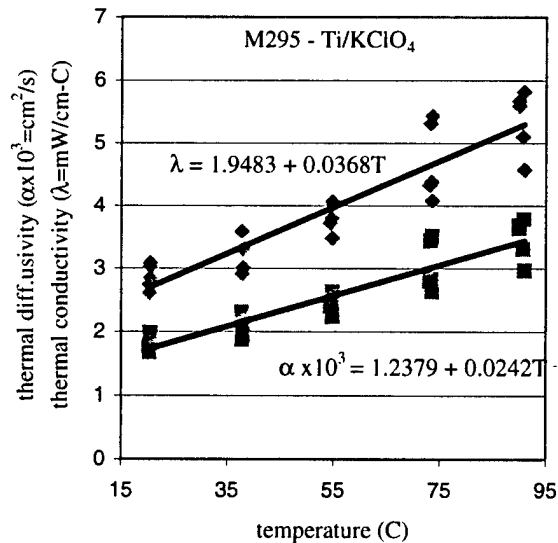


Figure 17. Thermal Diffusivity and Thermal Conductivity Measurements for Ti/ KClO_4 .

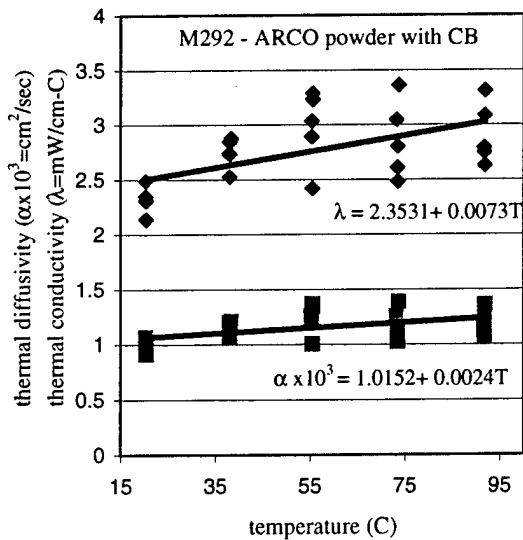


Figure 18. Thermal Diffusivity and Thermal Conductivity Measurements for an ARCO Formulation With 5-Weight-Percent Added Carbon Black.

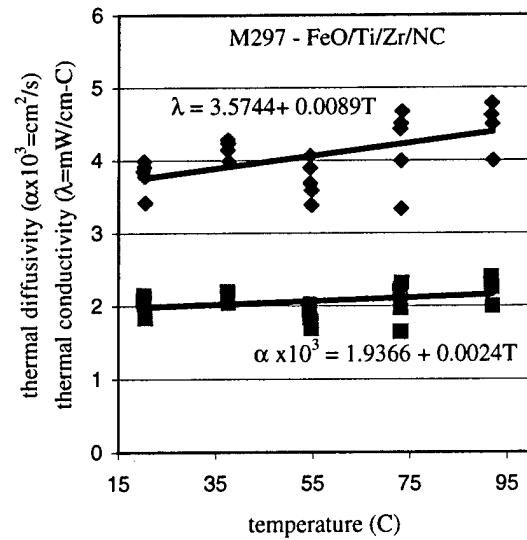


Figure 19. Thermal Diffusivity and Thermal Conductivity Measurements FeO/Ti/Zr/NC.

Table 2. Comparison of Thermal Transport Property Measurements at 23.5° C

| Material | Source | λ (mW/cm-C) | $\alpha \times 10^3$ (cm ² /s) | c_p (J/g-°C) |
|----------------------|-----------------------|------------------------|----------------------------------------------|-------------------|
| Black Powder | McQuaid and Beyer [5] | 3.3 | 2.5 | 0.8 |
| — | This work | 2.0 | 1.0 | 1.1 |
| B/KNO ₃ | McQuaid and Beyer [5] | 3.6 | 3.0 | 0.8 |
| — | This work | 1.2 | 0.7 | 1.1 |
| Zr/KClO ₄ | McQuaid and Beyer [5] | 4.8 | 3.4 | 0.5 |
| — | This work | 1.9 | 1.2 | 0.6 |
| Acrylic | Miller and Kotlar [2] | 1.8 | 1.1 | 1.3 |

maximum temperature will be at the surface ($x = 0$) for all t , the irradiance necessary to raise the temperature of the surface to the material's autoignition temperature under this set of assumptions may be calculated by setting x equal to zero and rearranging equation (4) to give

$$f_o = \sqrt{\frac{\pi}{4t}} \left(\sqrt{\lambda_b \rho_b c_{pb}} + \sqrt{\lambda_s \rho_s c_{ps}} \right) \Delta T, \quad (10)$$

where ΔT is the difference between the autoignition temperature and the ambient temperature. Expressed in this manner, the desirability of having materials with low (product) values of λ , ρ , and c_p is apparent. Moreover, this expression shows that the results presented in Figure 13 can be used directly in estimating flux requirements under the given set of assumptions.

To provide some appreciation of the ramifications of a material's thermal transport properties on the fluence required to ignite it, we assume that the results in Figure 13 can be extrapolated to the autoignition temperature for each compound and calculate the fluence needed to raise the temperature of the surface of each material from 25° C to its autoignition temperature in 0.5 s. (Again, 0.5 s is the maximum ignition time delay permitted for the GUFS application.) The results for three different cases are presented in Table 3. In Case A, it is assumed that the bounding window is a perfect insulator ($\lambda_b = 0$). In Case B, the bounding window is given the properties of acrylic. And, in Case C, the bounding window is given the properties of fused silica. (In each case, the thermal transport properties of the bounding window are assumed to be temperature independent.) For reference, 130 W/cm² is equal to 10 mW at the distal end of an optical fiber with a 100- μ m-diameter core—a value that would make laser-based ignition a viable option for the GUFS system. Except for the value for black powder computed assuming an autoignition temperature of 200° C, the differences between compounds for a given case are not considered significant. The difference between cases are notable, with the minimum fluence for Case B being approximately 50% higher than for Case A and the minimum fluence for Case C being approximately twice as high as Case A.

6. Summary

It has been recognized that the thermal transport properties of the igniter material in a laser-based ignition system will influence the minimum irradiance required to function a round [8]. However, the difficulty of obtaining reliable thermal transport property data,

Table 3. Minimum Fluence Required to Reach Autoignition Temperature Within 0.5 s

| Lot No. | Material | Case A (W/cm ²) | Case B (W/cm ²) | Case C (W/cm ²) |
|---------|-----------------------------------------|--------------------------------|--------------------------------|--------------------------------|
| M293 | Black Powder | 70 20 | 100 50 | 140 90 |
| M294 | B/KNO ₃ | 70 | 100 | 140 |
| M291 | Zr/KClO ₄ /VAAR ^a | 50 | 80 | 120 |
| M295 | Ti/KClO ₄ ^b | 80 | 110 | 150 |
| M297 | FeO/Ti/Zr/NC | 60 | 90 | 130 |
| M292 | ARCO w/ carbon black ^b | 50 | 80 | 120 |

^a Values for this material are based on its explosive temperature.

^b The autoignition temperature is unknown. A value of 450° C has been assumed for the calculations.

particularly for energetic materials, is a hurdle to quantifying the impact of this aspect of the energy transport process. The results of this study provide values for the thermal transport properties of six pyrotechnic compounds being considered for use in back-fitting a GUFS system with a laser-based ignition system. The results were obtained with an experimental technique developed specifically for the difficult case of acquiring such information from small, electrically conductive specimens with relatively low diffusivity values. In addition to this primary objective, DSC results for compounds containing red powder indicate that the thermal stability of this pyrotechnic may be an issue.

To begin to quantify the impact of thermal transport properties on irradiance requirements, the experimental results were employed as input to a model that assumes all the laser energy is absorbed at the surface, no phase changes or chemical reactions occur, and that thermal transport property measurements for each compound can be extrapolated to their autoignition temperature. While this model is a great oversimplification of the actual process, and thus of limited value for establishing minimum irradiance requirements for such systems, its predictions are consistent with expectations based on previous studies. Moreover, the results obtained for the different materials are instructive. In particular, they indicate that the differences in thermal properties of the candidates studied thus far will not be a significant factor from the standpoint of reducing fluence requirements. On the other hand, the packaging of the igniter material will be an important consideration.

7. References

1. Strakovsky, L., A. Cohen, R. Fifer, R. Beyer, and B. Forch. "Laser Ignition of Propellants and Explosives." ARL-TR-1699, U.S. Army Research Laboratory, Aberdeen Proving Ground, MD, 1998.
2. Miller, M. S., and A. J. Kotlar. "Technique for Measuring Thermal Diffusivity/Conductivity of Small Thermal Insulator Specimens." *Review of Scientific Instruments*, vol. 64, p. 2954, 1993.
3. Carslaw, H. S., and J. C. Jaeger. *Conduction of Heat in Solids*. Second edition, London: Oxford University Press, 1959.
4. Hui, A. K., B. H. Armstrong, and A. A. Wray. "Rapid Computation of the Voight and Complex Error Functions." *Journal of Quantitative Spectroscopy Radiation and Transfer*, vol. 19, p. 509, 1978.
5. McQuaid, M. J., and R. A. Beyer. "Irradiance Requirements for the Laser Ignition of Pyrotechnics: Thermal Conductivity and Thermal Diffusivity Considerations." *34th JANNAF Combustion Subcommittee Meeting*, 1997.
6. Wylie, C. R. *Advanced Engineering Mathematics*. Fourth edition, New York: McGraw-Hill, 1975.
7. Perry, R. H., and C. H. Chilton (editors). *Chemical Engineer's Handbook*, Fifth edition, New York: McGraw-Hill, 1973.
8. Kramer, D. P., E. M. Spangler, and T. M. Beckman. "Laser-Ignited Explosive and Pyrotechnic Components." *American Ceramic Society Bulletin*, vol. 72, p. 78, 1993.

INTENTIONALLY LEFT BLANK.

List of Symbols

Nomenclature

| | |
|------------|-----------------------------------------------------------------------------|
| α | thermal diffusivity (square centimeters/second) |
| λ | thermal conductivity (watts/centimeter•degrees Celsius) |
| ρ | density (grams/cubic centimeter) |
| A | area of the foil (square centimeters) |
| c_p | heat capacity (joules/gram•degrees Celsius) |
| E | activation energy in the Arrhenius heat release expression (joules/mole) |
| f_o | heat flux (watts/square centimeter) |
| $f^-(0,t)$ | heat flux into base (watts/square centimeter) |
| $f^+(0,t)$ | heat flux into sample (watts/square centimeter) |
| I_o | nominal current of electrical pulse employed to heat foil (amperes) |
| l | length (centimeters) |
| n | absorption coefficient |
| Q | heat of reaction |
| r_f | resistance of foil (ohms) |
| R | gas constant (joules/degrees Celsius•mole) |
| $R(t)$ | temporal response of passive system to a unit step forcing function |
| t | time (seconds) |
| T_o | ambient temperature (degrees Celsius) |
| $T(x,t)$ | actual temperature (degrees Celsius) |
| $u(t)$ | measured temperature (degrees Celsius) |
| x | distance from heat source (centimeters) |
| z | first order pre-exponential factor in the Arrhenius heat release expression |

Subscripts

| | |
|-----|------------------------|
| b | base material property |
| s | specimen property |

INTENTIONALLY LEFT BLANK.

NO. OF
COPIES ORGANIZATION

2 DEFENSE TECHNICAL
INFORMATION CENTER
DTIC DDA
8725 JOHN J KINGMAN RD
STE 0944
FT BELVOIR VA 22060-6218

1 HQDA
DAMO FDQ
D SCHMIDT
400 ARMY PENTAGON
WASHINGTON DC 20310-0460

1 OSD
OUSD(A&T)/ODDDR&E(R)
R J TREW
THE PENTAGON
WASHINGTON DC 20301-7100

1 DPTY CG FOR RDA
US ARMY MATERIEL CMD
AMCRDA
5001 EISENHOWER AVE
ALEXANDRIA VA 22333-0001

1 INST FOR ADVNCD TCHNLGY
THE UNIV OF TEXAS AT AUSTIN
PO BOX 202797
AUSTIN TX 78720-2797

1 DARPA
B KASPAR
3701 N FAIRFAX DR
ARLINGTON VA 22203-1714

1 NAVAL SURFACE WARFARE CTR
CODE B07 J PENNELLA
17320 DAHLGREN RD
BLDG 1470 RM 1101
DAHLGREN VA 22448-5100

1 US MILITARY ACADEMY
MATH SCI CTR OF EXCELLENCE
DEPT OF MATHEMATICAL SCI
MADN MATH
THAYER HALL
WEST POINT NY 10996-1786

NO. OF
COPIES ORGANIZATION

1 DIRECTOR
US ARMY RESEARCH LAB
AMSRL DD
J J ROCCHIO
2800 POWDER MILL RD
ADELPHI MD 20783-1197

1 DIRECTOR
US ARMY RESEARCH LAB
AMSRL CS AS (RECORDS MGMT)
2800 POWDER MILL RD
ADELPHI MD 20783-1145

3 DIRECTOR
US ARMY RESEARCH LAB
AMSRL CI LL
2800 POWDER MILL RD
ADELPHI MD 20783-1145

ABERDEEN PROVING GROUND

4 DIR USARL
AMSRL CI LP (BLDG 305)

NO. OF
COPIES ORGANIZATION

ABERDEEN PROVING GROUND

29 DIR USARL
AMSRL WM B
A W HORST
AMSRL WM BD
B E FORCH
W R ANDERSON
R A BEYER
S W BUNTE
C F CHABALOWSKI
S COLEMAN
A COHEN
R DANIEL
D DEVYNCK
R A FIFER
B E HOMAN
A JUHASZ
A J KOTLAR
K L MCNESBY
M MCQUAID (2 CPS)
M S MILLER
A W MIZIOLEK
J B MORRIS
J E NEWBERRY
R A PESCE-RODRIGUEZ
P REEVES
B M RICE
R C SAUSA
M A SCHROEDER
J A VANDERHOFF
AMSRL WM BE
A BIRK
C LEVERITT

| REPORT DOCUMENTATION PAGE | | | Form Approved OMB No. 0704-0188 | |
|----------------------------------------------------------------------------------------------------------------------------------------------------------------------------------------------------------------------------------------------------------------------------------------------------------------------------------------------------------------------------------------------------------------------------------------------------------------------------------------------------------------------------------------------------------------------------------------------------------------------------------------------------------------------------------------------------------------------------------------------------------------------------------------------------------------------------------------------------------------------------------------------------------------------------------------------------------------------------------------------------------------------------------------------------------------------------------------------------------------------------------------------------------------------------------------------------------------------------------------------------------------------------------------------------------------------------------------------------------------------------------------------------------------------------------------------------------------------------------------------------------------------------------------------------------------------------------------------------------|-------------------------------------------------------------|------------------------------------------------------------|------------------------------------------------------------|----------------------------------------------------------------------|
| Public reporting burden for this collection of information is estimated to average 1 hour per response, including the time for reviewing instructions, searching existing data sources, gathering and maintaining the data needed, and completing and reviewing the collection of information. Send comments regarding this burden estimate or any other aspect of this collection of information, including suggestions for reducing this burden, to Washington Headquarters Services, Directorate for Information Operations and Reports, 1215 Jefferson Davis Highway, Suite 1204, Arlington, VA 22202-4302, and to the Office of Management and Budget, Paperwork Reduction Project(0704-0188), Washington, DC 20503. | | | | |
| 1. AGENCY USE ONLY (Leave blank) | | 2. REPORT DATE August 1999 | | 3. REPORT TYPE AND DATES COVERED Final, March 1997 - October 1998 |
| 4. TITLE AND SUBTITLE Laser-Based Ignition for a Gunfire Simulator (GUFS): Thermal Transport Properties for Candidate Igniter Materials | | | 5. FUNDING NUMBERS 1L161102AH43 | |
| 6. AUTHOR(S) M. J. McQuaid, A. E. Kinkennon, R. A. Pesce-Rodriguez, and R. A. Beyer | | | | |
| 7. PERFORMING ORGANIZATION NAME(S) AND ADDRESS(ES) U.S. Army Research Laboratory ATTN: AMSRL-WM-BD Aberdeen Proving Ground, MD 21005-5066 | | | 8. PERFORMING ORGANIZATION REPORT NUMBER ARL-TR-2033 | |
| 9. SPONSORING/MONITORING AGENCY NAMES(S) AND ADDRESS(ES) | | | 10. SPONSORING/MONITORING AGENCY REPORT NUMBER | |
| 11. SUPPLEMENTARY NOTES | | | | |
| 12a. DISTRIBUTION/AVAILABILITY STATEMENT Approved for public release; distribution is unlimited. | | | 12b. DISTRIBUTION CODE | |
| 13. ABSTRACT (Maximum 200 words) This report presents the results of a study undertaken to help build a database and modeling capability that will support the design of a laser-based ignition system for a gun-fire simulation (GUFS) platform. In this study, the thermal transport properties of pressed pellets of candidate igniter materials were experimentally investigated in the range 20–100° C via (1) the technique developed by Miller and Kotlar ("Technique for Measuring Thermal Diffusivity/Conductivity of Small Thermal Insulator Specimens," <i>Review of Scientific Instruments</i> , vol. 64, p. 2954, 1993) and (2) a small modification to their technique that allows it to be used for (slightly) electrically conductive materials. The compounds investigated in this manner include black powder, red powder (with and without 0.5-weight-percent carbon black), B/KNO ₃ , A1A, Zr/KClO ₄ , Ti/KClO ₄ , an ARCO formulation (with 0.5-weight-percent carbon black), and an FeO/Ti/Zr/NC mixture. In addition, the heat capacities of these compounds were determined over the range 20–100° C via differential scanning calorimetry. The experimentally derived parameters are employed as input to a simplified model of the heat-transfer process attending the irradiation of a candidate with a relatively low-fluence laser beam. The results indicate that the differences in the thermal transport properties of the materials studied will not lead to significant differences in the irradiance required to ignite them. | | | | |
| 14. SUBJECT TERMS thermal conductivity, laser ignition, pyrotechnics | | | 15. NUMBER OF PAGES 32 | |
| | | | 16. PRICE CODE | |
| 17. SECURITY CLASSIFICATION OF REPORT UNCLASSIFIED | 18. SECURITY CLASSIFICATION OF THIS PAGE UNCLASSIFIED | 19. SECURITY CLASSIFICATION OF ABSTRACT UNCLASSIFIED | 20. LIMITATION OF ABSTRACT UL | |

INTENTIONALLY LEFT BLANK.

USER EVALUATION SHEET/CHANGE OF ADDRESS

This Laboratory undertakes a continuing effort to improve the quality of the reports it publishes. Your comments/answers to the items/questions below will aid us in our efforts.

1. ARL Report Number/Author ARL-TR-2033 (McQuaid) Date of Report August 1999

2. Date Report Received _____

3. Does this report satisfy a need? (Comment on purpose, related project, or other area of interest for which the report will be used.) _____

4. Specifically, how is the report being used? (Information source, design data, procedure, source of ideas, etc.) _____

5. Has the information in this report led to any quantitative savings as far as man-hours or dollars saved, operating costs avoided, or efficiencies achieved, etc? If so, please elaborate. _____

6. General Comments. What do you think should be changed to improve future reports? (Indicate changes to organization, technical content, format, etc.) _____

CURRENT
ADDRESS

Organization

Name

E-mail Name

Street or P.O. Box No.

City, State, Zip Code

7. If indicating a Change of Address or Address Correction, please provide the Current or Correct address above and the Old or Incorrect address below.

OLD
ADDRESS

Organization

Name

Street or P.O. Box No.

City, State, Zip Code

(Remove this sheet, fold as indicated, tape closed, and mail.)
(DO NOT STAPLE)